International Conference on Computational Science, ICCS 2017, 12-14 June 2017, Zurich, Switzerland

An observable regularization of compressible two-phase flow

Bahman Aboulhasanzadeh[1] and Kamran Mohseni[1*]

University of Florida, Florida, U.S.A.
mohseni@ufl.edu

Abstract

Many fluid flow problems involving turbulence, shocks, and material interfaces create a common issue high wave number irregularity. The non-linear advection term in the governing equations for all of these problems keep generating higher wave modes as k goes to infinity. In this work, we present an inviscid regularization technique, called observable regularization, for the simulation of two-phase compressible flow. In this technique, we use observable divergence theorem to derive an observable equation for tracking material interface (volume fraction). In some one-dimensional test cases, first we show that this method preserves pressure equilibrium at material interface, then we compare our results to exact Euler solutions. At the end we demonstrate a two-dimensional simulation of shock-bubble interaction showing good agreement with available experimental data from literature.

Keywords: Observable divergence, two-phase flow, compressible flow, shock-bubble interaction

1 Introduction

Material interfaces and/or shockwaves are the source of complex flow behavior in many fluid engineering problems. Scientific understanding of these problems is the base for technological advances needed in engineering and daily life. For example, shock-induced collapse is a damaging phenomena leading to propeller erosion in naval engineering; similar mechanisms may lead to tissue damage and internal bleeding in shockwave lithotripsy, a non-invasive medical treatment of kidney stone. In the past couple of decades, with the improvement of computational power, numerical study of such problems became mainstream. While solving the conservation equations needs considerable understanding of the equations, appearance of sharp variations or discontinuity in flow variables create challenges that need specific attention.

In the past three decades, a large amount of effort is gone into numerical treatment of material interfaces and shocks. Many approaches are developed for tracking/capturing interfaces including Front Tracking [3], γ-based model [15], mass fraction based model [22], volume fraction based model [1], and level set-ghost fluid method [7]. On the other hand, several Riemann solver type approaches are developed for physical approximation of fluxes at discontinuities,

---

*Phone: +1(352)273-1834

specifically for problems including shock waves; Roe solver [23], HLL [11], HLLC [27], and flux vector splitting [26] are a small sample of such methods. All the efforts in solving fluid equations are based on the *assumption* that Euler set of conservation equations are valid when solved with limited resolution. This assumption holds in regions of smooth variations where the flow variables and their derivatives can be represented using the limited resolution with minimal error. However, it may not be the case in regions with sharp changes.

When we have sharp variations in a field quantity, one needs to have a large number of wave modes in the Fourier space to correctly represent the data and as thickness of jump decreases, the required number of modes approaches infinity. Using the Euler set of equations, we inherit the infinite resolution assumption used in their derivation. Then, by discretizing the domain into finite sizes we violate that assumption. This leads to numerical instability challenges in simulation of shocks, interfaces, and even turbulence. In order to avoid this conflict, Mohseni [20, 17] developed the concept of *Observable Divergence* in which the finite resolution limit (observability limit) is introduced into the derivation of conservation equations. Using observable divergence mandate a reevaluation of the governing equations for the existing problems in order to systematically resolve the challenges in the simulations of fluid flows, including but not limited to multiphase flows, shocks, and turbulence.

In this paper, we first develop observable version of the governing equations for a two-phase flow problem. Without loosing generality and for the sake of simplicity, we use a gas-gas problem for which we can use ideal gas equation of state. Then we show solution of 1D and 2D shock-interface interaction problems using observable set of equations and compare them to available exact solution or experimental results from literature. We also investigate the effect of observability limit on the results.

2   Observability

Solving fluid dynamics equations often require treating non-linear terms. The challenge with nonlinear terms is in the way that they can create discontinuity in the flow field even starting from a smooth initial condition. Computational challenges in simulation of multiphase flow, shock, and turbulence can be viewed as separate problems as one can see in the literature. However, if we look at the problem in the Fourier space, they are all the symptoms of one main issue, the finite available resolution, or as we call it, the limit of observability. To put it in context, observing Burgers equation, $u_t + uu_x = 0$, with a smooth initial condition, $u = sin(x)$ with $x \in [0, 2\pi)$, initially u can be represented using one Fourier mode. The nonlinear term uu_x represent a convolution in Fourier space, which means at each time step the number of non-zero Fourier modes in the solution increases. Consequently, in a finite time, the number of available modes in the solution, m, will be larger than the available number of modes in any computational simulation, n, as a result of finite resolution. When m becomes greater than n the energy cascade from low wave numbers to higher wave numbers are not correctly calculated and a phenomena called spectral blocking contaminate the solution and brings the tail of spectral energy up as shown using the dash-dot line in Fig. 1. The beginning of spectral blocking is the time when the instability in the solution start to grow and if not controlled, the solution would diverge in a short time. Significant effort is gone into controlling numerical instabilities in fluid flow computations depending on the problem of interest. Examples of such efforts includes, diffused interface in incompressible multiphase flow, Riemann solvers in compressible flow, and turbulence modeling using RANS or LES in turbulent flows. In these approaches, the starting points are equations with infinite observability, which means dx can go to zero. However, since in practice Δx in numerics cannot go to zero and also in most cases the
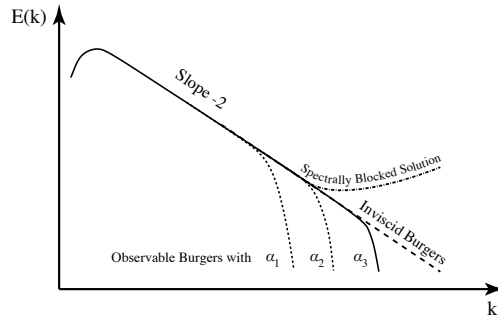
Figure 1: Schematic of energy cascade from low wave modes to higher wave modes is shown for inviscid burgers' equation with infinite resolution (green long-dashed line), observable burgers' equation with different limit of observability α_1, α_2, and α_3 with $\alpha_1 > \alpha_2 > \alpha_3$ (black dashed or solid lines), spectrally-blocked solution of inviscid burgers' equation (red dash-dot line).

large scale features of flow is of interest to scientists and engineers, the equations are averaged in different ways to achieve equations for capturing main features of the flow. These averaging techniques generate extra terms in the system of equations which need some kind of modeling.

A different way to look at the problem is to use the finite resolution assumption when deriving the governing equation as shown in the derivation of observable divergence theorem by [17]. For a vector field, $\mathbf{F} = f\mathbf{V}$, we define the observable divergence, *odiv*, using

$$odiv\,\mathbf{F} = \overline{f}\nabla\cdot\mathbf{V} + \overline{\mathbf{V}}\cdot\nabla f, \tag{1}$$

where $(\bar{\cdot})$ is an averaging operator with an observability of length scale α. Without loosing generality, here we use a Helmholtz filter as the averaging operator defined by,

$$f = \overline{f} - \alpha^2\nabla^2\overline{f}. \tag{2}$$

Observable divergence theorem for a region of space, Ω, surrounded by a surface, S, states that

$$\iiint_\Omega odiv\,\mathbf{F}dV = \iiint_\Omega (\overline{f}\nabla\cdot\mathbf{V} + \overline{\mathbf{V}}\cdot\nabla f)dV = \iint_S \mathbf{F}\cdot\mathbf{n}dS, \tag{3}$$

where $\mathbf{n}$ is the normal vector to the surface. Using this theorem, we can easily rewrite the conservation laws with finite resolution assmption, described in the following section.

3   Governing equations

For the equation of motion, we start with the conservation of mass, momentum, and energy for the mixture fluid properties used in [14] which are inferred in different ways [1, 18] from Baer-Nunziato 1986 model [2] or Drew's derivation of two phase conservation equations [5, 6]:

$$\frac{\partial\rho}{\partial t} + \nabla\cdot\rho\mathbf{u} = 0, \tag{4}$$

$$\frac{\partial\rho\mathbf{u}}{\partial t} + \nabla\cdot\rho\mathbf{u}\mathbf{u} + \nabla p = 0, \tag{5}$$

$$\frac{\partial\rho E}{\partial t} + \nabla\cdot(\rho E\mathbf{u} + p\mathbf{u}) = 0, \tag{6}$$

3

where ρ, $\mathbf{u}$, p, and E are density, velocity vector, pressure and specific total energy of fluid mixture, respectively. In the derivation of Equations (4) to (6), an instantaneous mechanical relaxation between phases is assumed, $u = u_1 = u_2$ and $p = p_1 = p_2$ where subscript 1 and 2 refer to phase 1 and 2. The mixture quantities are defined using the following relations:

$$\rho = \rho_1 z_1 + \rho_2 z_2, \quad \rho E = \rho_1 E_1 z_1 + \rho_2 E_2 z_2, \tag{7}$$

here, z_1 and z_2 are the volume fractions of phase 1 and 2 and $z_1 + z_2 = 1$. In the rest of this text z with no subscript refers to z_1.

By writing Equations (4) to (6) in integral form and then using the observable divergence theorem to replace surface fluxes with the *odiv* of those fluxes, we obtain the observable version of the conservation equations for the fluid mixture

$$\frac{\partial \rho}{\partial t} + \overline{\rho} \nabla \cdot \mathbf{u} + \overline{\mathbf{u}} \cdot \nabla \rho = 0, \tag{8}$$

$$\frac{\partial \rho \mathbf{u}}{\partial t} + \overline{\rho \mathbf{u}} \nabla \cdot \mathbf{u} + \overline{\mathbf{u}} \cdot \nabla \rho \mathbf{u} + \nabla p = 0, \tag{9}$$

$$\frac{\partial \rho E}{\partial t} + \overline{\rho E} \nabla \cdot \mathbf{u} + \overline{\mathbf{u}} \cdot \nabla \rho E + \overline{p} \nabla \cdot \mathbf{u} + \overline{\mathbf{u}} \cdot \nabla p = 0. \tag{10}$$

In order to close this system of equations, an equation of state (EOS) needs to be used. Without loosing generality, here we use ideal gas equation of state,

$$\rho E - \frac{1}{2} \rho \mathbf{u}^2 = \Gamma p, \ \Gamma = \frac{1}{\gamma - 1}, \tag{11}$$

where γ is the ratio of specific heat of fluid mixture at constant pressure to its specific heat at constant volume. The mixture Γ is defined as

$$\Gamma = \frac{1}{\gamma - 1} = \frac{z_1}{\gamma_1 - 1} + \frac{z_2}{\gamma_2 - 1}. \tag{12}$$

In order to calculate Γ, volume fraction of one of the phases should be known. To this end, we need an equation for volume fraction which is derived in the following subsection.

3.1 Observable interface capturing

For the purpose of capturing the interface while keeping pressure equilibrium at the interface, we consider the case of interface only problem, following [24], in which velocity and pressure are constant in the domain while density and material properties changes across the interface. For simplicity, we present the one-dimensional equations. Equations (8) to (10) can be rewritten in the following non-conservative form,

$$\frac{\partial \rho}{\partial t} + \bar{\rho} \frac{\partial u}{\partial x} + \overline{u} \frac{\partial \rho}{\partial x} = 0, \tag{13}$$

$$\rho \frac{\partial u}{\partial t} + \overline{\rho u} \frac{\partial u}{\partial x} + (\overline{u} - u) \frac{\partial \rho u}{\partial x} + \frac{\partial p}{\partial x} = 0, \tag{14}$$

$$\frac{\partial \rho e}{\partial t} + \overline{\rho e} \frac{\partial u}{\partial x} + \bar{u} \frac{\partial \rho e}{\partial x} + \bar{p} \frac{\partial u}{\partial x} + (\overline{u} - u) \frac{\partial p}{\partial x} + \frac{1}{2} \left(\overline{\rho u^2} - 2u \overline{\rho u} + \overline{u} \rho u \right) \frac{\partial u}{\partial x}$$
$$+ \frac{1}{2} \left(u^2 - u \bar{u} \right) \frac{\partial \rho u}{\partial x} = 0, \tag{15}$$

where e is the specific internal energy with $E = e + \frac{1}{2}u^2$. Using the assumptions mentioned above, the equations for the evolution of interface can be inferred to be

$$\frac{\partial \rho}{\partial t} + \overline{u}\frac{\partial \rho}{\partial x} = 0, \tag{16}$$

$$\frac{\partial \rho e}{\partial t} + \overline{u}\frac{\partial \rho e}{\partial x} = 0. \tag{17}$$

By inserting equation of state into Eq. (17) and rearranging we have

$$\Gamma\left(\frac{\partial p}{\partial t} + \overline{u}\frac{\partial p}{\partial x}\right) + p\left(\frac{\partial \Gamma}{\partial t} + \overline{u}\frac{\partial \Gamma}{\partial x}\right) = 0. \tag{18}$$

With pressure equilibrium requirement, the first parenthesis is zero. Since this equation needs to be satisfied for any pressure, the term in the second parentheses should be zero. Writing second parenthesis using Eq. (12), the simplified equation is

$$\frac{\partial z_1}{\partial t} + \overline{u}\frac{\partial z_1}{\partial x} = 0,$$

which is the observable equation for capturing material interface in one-dimension and the general form of the equation is

$$\frac{\partial z_1}{\partial t} + \overline{\mathbf{u}} \cdot \nabla z_1 = 0. \tag{19}$$

3.2   Numerical method

In this work, we use a pseudo-spectral discretization of the derivatives in order to avoid any numerical dissipation contaminating the results. Helmholtz operator, Eq. (2), is also applied in the Fourier space to calculate the observed quantities. A buffer zone is added to the sides of the physical domain to

1. make the computational domain periodic,

2. make transition from the condition on the right of the physical domain to left of it,

3. prevent reflection of waves from boundaries and into the domain.

To achieve the second condition while satisfying the third condition we use a smooth 5th order polynomial as a weighting function to transition from the governing equation in the physical domain to a linear advection equation with a damping term in the buffer zone. The governing equation in the buffer zone is applied using similar ideas proposed by [8]. A 3rd order TVD Runge-Kutta method is used for time marching [9]. For dealiasing, a low pass exponential filter, $H(k) = \exp(-36|k/k_{\max}|^{36})$, is used [12]. For all initial conditions we use double filtering as explained by [21].

4   Results and discussion

Here, we present several 1D test cases to show the performance of the proposed method compared to other available methods and demonstrate the effect of observability limit. We also present a 2D computation to show that the observable set of equations for two phase flow correctly predict available experimental results.

1D Advection of isolated interface

First, we examine an isolated interface in a one-dimensional domain, with periodic boundary condition and the initial condition defined by:

$$(\rho, u, p, \gamma) = \begin{cases} (1, 0.5, 1/1.4, 1.4) & -1 \leqslant x < 0, \\ (10, 0.5, 1/1.4, 1.2) & 0 \leqslant x < 1. \end{cases} \tag{20}$$

Figure 2 shows the result at time equal 4 when all the flow variables should be exactly equal to initial condition. Observed (filtered) density and ratio of heat capacities are shown using blue empty circles which are in good agreement with the two-phase Euler's exact solution (black solid lines). In addition, we include the results of a WENO5 finite volume method calculated by [14] (orange empty triangles). The magnitude of differences between the final and initial observed velocity and pressure are demonstrated to be zero to the order of machine precision, as expected. This shows that our method preserves the pressure equilibrium at material interfaces. Here we use grid size $\Delta x = 0.01$ similar to [14] and we set non-dimensional observability limit $\alpha/\Delta x = 1$.
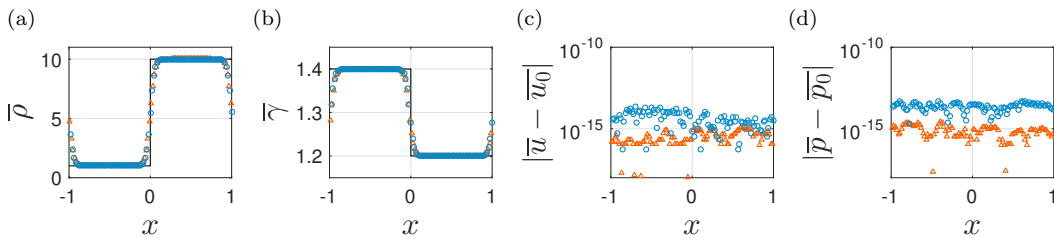

Figure 2: Solution of isolated interface problem using observable two-phase Euler equation (blue empty circles) compared to the exact solution of two-phase Euler (black solid lines) and solution of two-phase Euler problem using a WENO5 finite volume method, [14], (red empty triangles). (a) mixture density, $\bar{\rho}$, (b) ratio of specific heat, γ, (c) magnitude of difference between final and initial velocity, and (d) magnitude of difference between final and initial pressure are shown here.

1D interaction of a shock wave with a Helium bubble

In this problem which is studied by [22], a Mach 1.22 shock wave traveling in air interacts with a Helium bubble. The initial condition for this problem is:

$$(\rho_1 z, \rho_2 (1-z), u, p, z) = \begin{cases} (1.3764, 0, 0.3947, 1.5698, 1) & 0 \leq x < 0.25, \\ (1, 0, 0, 1, 1) & 0.25 \leq x < 0.4, \\ (0, 0.138, 0, 1, 0) & 0.4 \leq x < 0.6, \\ (1, 0, 0, 1, 1) & 0.6 \leq x < 1. \end{cases} \tag{21}$$

The ratio of specific heat, γ, is set to 1.67 and 1.4, inside ($z = 0$) and outside ($z = 1$) the bubble, respectively. Figure 3 demonstrate the results for this problem at $t = 0.35$. The solid black line is the reference result using a high resolution of 16384 grid points and $\alpha/\Delta x = 1.5$. The red dotted line and blue dash-dot line are simulations using a 1024 grid points with $\alpha/\Delta x$ equal 1.5 and 4.5, respectively.

When the incident shock hits the interface, a left going rarefaction wave reflects while a shock passes into the bubble. This shock hits the other end of bubble and creates a transmitted shock and a reflected shock. These interactions consequently results in two left going and three right going shock waves until $t = 0.35$. As shown in the figure, for this problem the method can regularize the equation using a non-dimensional observability limit as small as 1.5. Obviously,

as we increase $\alpha/\Delta x$, the equations become more regularized but at the same time we loose details of our quantities of interest. So, the general rule of thumb for selecting $\alpha/\Delta x$ is to be as close as possible to 1 to retain the details as much as possible. While, choosing $\alpha/\Delta x$ less than one might be possible, there is a risk for computations to diverge since we are under critical observability limit which is of order Δx. This risk increases as the severity of discontinuity in the initial condition increases.
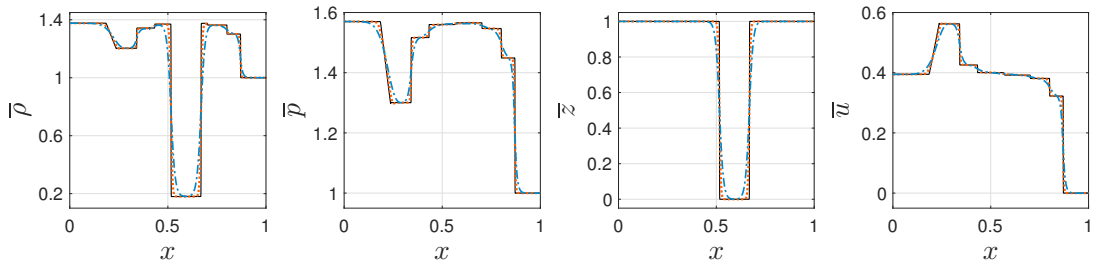

Figure 3: Plot of observed density, pressure, volume fraction, and velocity for a shock-Helium bubble interaction at $t = 0.35$ with initial condition given by Eq. (21). Solid line is done using a high resolution simulation with 16384 grid point with $\alpha/\Delta x = 1.5$, included as reference solution. Blue dash-dot line and red dotted line are simulations with 1024 grid points using $\alpha/\Delta x$ of 4.5 and 1.5, respectively.

1D interaction of a strong shock wave with air bubble

As stated by [4], the interaction of shock with a material interface can challenge numerical methods which does not solve the equations in conservative form. The main known artifact could be error in the resulting wave speeds which deteriorate as time passes and error in mass conservation increases. To investigate the performance of our method in this regard, we study the interaction of a strong shock wave with a material interface.

This problem is originally proposed by [16], and then a modified form of it, as used here, is solved by [13] and [4]. In this problem a Mach 8.96 shockwave moving in Helium interacts with an air bubble. Initially, the unshocked region has a small velocity towards the shock. We use the same resolution as [4], $\Delta x = 0.005$, with a non-dimensional observability limit $\alpha/\Delta x = 1$. The initial condition is:

$$(\rho_1 z, \rho_2(1-z), u, p, z) = \begin{cases} (0.386, 0, 26.59, 100, 1) & -1 \leq x < -0.8, \\ (0.1, 0, -0.5, 1, 1) & -0.8 \leq x < -0.2, \\ (0, 1, -0.5, 1, 0) & -0.2 \leq x < 1. \end{cases} \qquad (22)$$

Figure 4 shows good agreement between our results and exact solution of two-phase Euler and demonstrate that all the wave velocities are captured correctly. Since we are using pseudo-spectral method to calculate derivatives, any sharp changes needs to be taken place over several grid point in order to avoid Gibbs phenomena. As a result of strong shock, using a non-dimensional observability limit less than one creates spurious oscillations in the result. Using the Helmholtz filter, the observability limit imposes the shock thickness of about 4.6α (which here translates to about 5 cells or 6 grid points), as shown by [21].

2D interaction of a shock wave with a Refrigerant 22 bubble

This problem is a two-dimensional counterpart of the second case study solved in this section; a Mach 1.22 shockwave in the air interacting with a cylindrical Refrigerant 22 (R22) bubble with $\gamma = 1.249$ and $\rho_{R22} = 3.712$. This problem is first done experimentally by [10] and soon became a benchmark for numerical methods since it has complex wave interactions and also contains a Richtmyer-Meshkov instability that poses a severe challenge on computational methods. This
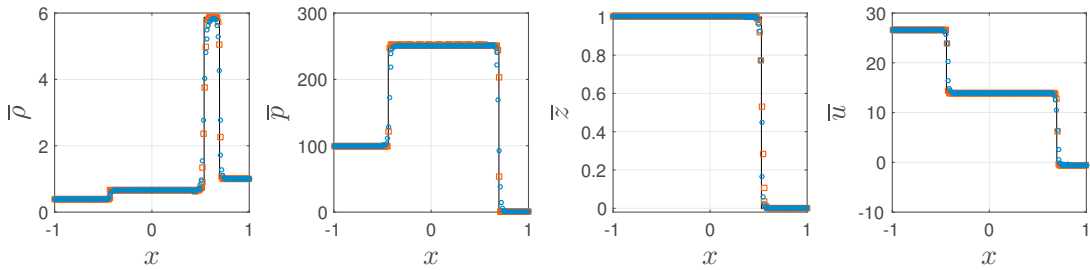
Figure 4: Plot of observed density, pressure, volume fraction, and velocity for a shock-bubble interaction at $t = 0.07$ with initial condition given by Eq. (22). Blue empty circles show the result with the presented method, red empty triangles show the results calculated using a WENO5 finite volume method presented by [4], and solid lines show the exact solution of two-phase Euler.

simulation is done using a grid resolution of $\Delta x = 0.111\,mm$ and a non-dimensional observability limit $\alpha/\Delta x = 2$. For plotting numerical schlieren results, we use the visualization technique introduced by [22]. Figure 5 shows the schematic of the problem setup in addition to schlieren images from [10] compared to numerical schlieren from our results. In vertical direction the domain is periodic. Since the problem is symmetric with respect to the horizontal axis through the center of bubble, the periodicity act like a reflective boundary condition on top and bottom edges.

The results in Figure 5 show good agreement between experimental and simulation snapshots. There are some minor differences in wave speeds that specifically can be seen in part (c) and (d) of the figures. Similar differences can be seen in [22, 25, 19]. These can be associated to material properties used in the numerical simulations in contrast to material properties in the experiment. The other source of these differences could be the way the material in the interface region is defined and the effect it has on the propagation of the waves.

5 Conclusion

In this work we used the concept of observability and observable divergence, [17], to develop a method for simulation of two-phase compressible flows. We developed an observable equation for tracking the material interface which preserve pressure equilibrium at the interface. A pseudo-spectral method is used since it does not have any numerical dissipation. This way we show that it is the system of equations that regularize the evident discontinuities in the problem and not numerical dissipation. Several 1D and 2D case studies are investigated and the results are compared with exact solutions of Euler or available experimental data. In all the cases the result from our method shows good agreement with the reference benchmark. We also looked at the effect of observability limit and explained the best practices for selecting the optimum observability limit parameter.
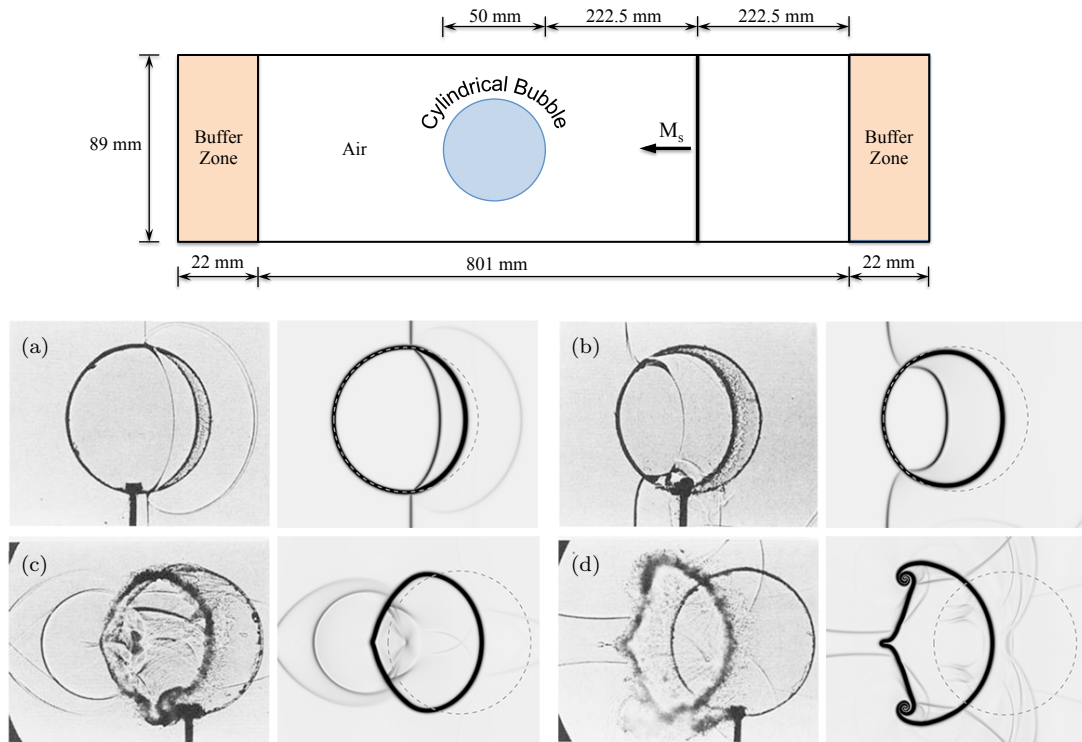
Acknowledgment

Figure 5: Schematic of the shock-bubble problem and schlieren snapshots of the interaction of a $M_s = 1.22$ shock in air hitting a cylindrical Refrigerant 22 (R22) bubble. The right frame of each subfigure shows the numerical schlieren of observable simulations while the left frames show the experimental snapshots from [10]. The snapshots are taken at times (a) 55 μs, (b) 115 μs, (c) 247 μs, and (d) 417 μs. The dashed line in numerical schlieren and solid circular line in experimental ones are the initial position of the bubble.

References

[1] G. Allaire, S. Clerc, and S. Kokh. A five-equation model for the simulation of interfaces between compressible fluids. *Journal of Computational Physics*, 181(2):577–616, 2002.

[2] M. R. Baer and J. W. Nunziato. A two-phase mixture theory for the deflagration-to-detonation transition (DDT) in reactive granular materials. *International Journal of Multiphase Flow*, 12(6):861–889, 1986.

[3] I. L. Chern, J. Glimm, O. McBryan, B. Plohr, and S. Yaniv. Front tracking for gas dynamics. *Journal of Computational Physics*, 62(1):83–110, 1986.

[4] V. Coralic and T. Colonius. Finite-volume WENO scheme for viscous compressible multi-component flows. *Journal of Computational Physics*, 274:95–121, 2014.

[5] D. A. Drew. Averaged field equations for two-phase media. *Studies in Applied Mathematics*, 50(2):133–166, 1971.

[6] D. A. Drew. Mathematical modeling of two-phase flow. *Annual Review of Fluid Mechanics*, 15:261–291, 1983.

[7] R. P. Fedkiw, T. Aslam, B. Merriman, and S. Osher. A non-oscillatory Eulerian approach to interfaces in multimaterial flows (the Ghost Fluid Method). *Journal of Computational Physics*, 152(2):457–492, 1999.

[8] J. B. Freund. Proposed inflow/outflow boundary condition for direct computation of aerodynamic sound. *AIAA Journal*, 35(10):740–742, 1997.

[9] S. Gottlieb and C.-W. Shu. Total variation diminishing Runge-Kutta schemes. *Mathematics of Computation*, 67(221):73–85, 1998.

[10] J. F. Haas and B. Sturtevant. Interaction of weak shock waves with cylindrical and spherical gas inhomogeneities. *Journal of Fluid Mechanics*, 181:41–76, 1987.

[11] A. Harten, P. D. Lax, and B. van Leer. On upstream differencing and Godunov-type schemes for hyperbolic conservation laws. *SIAM Review*, 25(1):35–61, 1983.

[12] T. Y. Hou and R. Li. Computing nearly singular solutions using pseudo-spectral methods. *Journal of Computational Physics*, 226(1):379–397, 2007.

[13] E. Johnsen. *Numerical simulations of non-spherical bubble collapse.* PhD thesis, California Institute of Technology, 2007.

[14] E. Johnsen and T. Colonius. Implementation of WENO schemes in compressible multicomponent flow problems. *Journal of Computational Physics*, 219(2):715–732, 2006.

[15] S. Karni. Multicomponent flow calculations by a consistent primitive algorithm. *Journal of Computational Physics*, 112(1):31–43, 1994.

[16] T. G. Liu, B. C. Khoo, and K. S. Yeo. Ghost fluid method for strong shock impacting on material interface. *Journal of Computational Physics*, 190(2):651–681, 2003.

[17] K. Mohseni. Observable divergence theorem: Evolution equations for inviscid regularization of shocks and turbulence. *arXiv preprint arXiv:1010.2612*, 2010.

[18] A. Murrone and H. Guillard. A five equation reduced model for compressible two phase flow problems. *Journal of Computational Physics*, 202(2):664–698, 2005.

[19] J. H. J. Niederhaus, J. A. Greenough, J. G. Oakley, D. Ranjan, M. H. Anderson, and R. Bonazza. A computational parameter study for the three-dimensional shock-bubble interaction. *Journal of Fluid Mechanics*, 594:85124, 2008.

[20] G. Norgard and K. Mohseni. An inviscid regularization of the one-dimensional Euler equations. In *Proceedings of the AIAA Fluid Dynamics Conference*, number 2009-3567, San Antonio, TX, USA, June 22-25 2009.

[21] G. Norgard and K. Mohseni. A new potential regularization of the one-dimensional Euler and homentropic Euler equations. *SIAM Journal of Multiscale Modeling and Simulation*, 8(4):1212–1242, 2010.

[22] J. J. Quirk and S. Karni. On the dynamics of a shockbubble interaction. *Journal of Fluid Mechanics*, 318:129–163, 1996.

[23] P. L. Roe. Approximate Riemann solvers, parameter vectors, and difference schemes. *Journal of Computational Physics*, 43(2):357–372, 1981.

[24] K.-M. Shyue. An efficient shock-capturing algorithm for compressible multicomponent problems. *Journal of Computational Physics*, 142(1):208–242, 1998.

[25] K.-M. Shyue. A wave-propagation based volume tracking method for compressible multicomponent flow in two space dimensions. *Journal of Computational Physics*, 215(1):219–244, 2006.

[26] J. L. Steger and R. F. Warming. Flux vector splitting of the inviscid gasdynamic equations with application to finite-difference methods. *Journal of Computational Physics*, 40(2):263–293, 1981.

[27] E. F. Toro, M. Spruce, and W. Speares. Restoration of the contact surface in the HLL-Riemann solver. *Shock Waves*, 4(1):25–34, 1994.